

61.6: Pressure sensor based on distributed temperature sensing

J.J. van Baar, R.J. Wiegerink, J.W. Berenschot, T.S.J. Lammerink, G.J.M. Krijnen and M. Elwenspoek

MESA⁺ Research Institute, University of Twente
P.O. Box 217, 7500 AE Enschede, The Netherlands
e-mail: J.vanBaar@el.utwente.nl fax: +31-53-489 3343

Abstract—

A differential pressure sensor has been realized with thermal readout. The thermal readout allows simultaneous measurement of the membrane deflection due to a pressure difference and measurement of the absolute pressure by operating the structure as a Pirani pressure sensor. The measuring of the temperature distribution makes it possible to take the heat transfer to the support in account and make the measurements independent of the temperature coefficient of resistance of the sensing elements.

Keywords— Pirani, pressure, thermal, mechanical, distributed, temperature, sensing

I. INTRODUCTION

TWO distinct classes of pressure sensors are formed on one hand by bending membrane pressure sensors, where a pressure difference results in a membrane deflection, and on the other hand by thermal pressure sensors, where the thermal conductivity of a gas is used as a measure for the absolute pressure [1]. In this paper a sensor is presented, which combines these two measurement principles. As a result, the sensor can be used for simultaneous measurement of a pressure difference and the absolute pressure.

In the case of bending membrane pressure sensors, the membrane deflection is usually measured using a change in electrical capacitance or by integrating strain gauges in the membrane. An alternative is to measure the thermal conductance between the membrane and a heat sink placed at a close distance. This was demonstrated in [2], where a heater was integrated on the membrane and the membrane temperature was measured using thermopiles. The heat sink was realized by bonding a second wafer on top of the wafer containing the membrane. The distance between the heated membrane and heat sink was in the order of 10 μm .

The sensor presented in this paper has a much smaller distance between membrane and heat sink, which is essential for using the structure to measure absolute pressure levels around atmospheric pressure. Furthermore, the sensor can be realized in a simple and reliable fabrication process based on etching of a sacrificial poly-Si

layer between two silicon nitride layers [3], [4].

Some first results of such a combined Pirani/bending membrane pressure sensors were presented in [5]. In this paper an improved sensor is presented, where the temperature distribution is measured in stead of the mean temperature. The advantages are the possibility to take the heat transfer to the support in account and making the measurement independent of the Temperature Coefficient of Resistance.

II. OPERATION PRINCIPLE

Figure 1 shows the basic structure of the sensor. It consists of a circular silicon nitride membrane positioned 1 μm above the silicon substrate. A channel connects the cavity below the membrane with a hole at the backside of the wafer. Thus, a pressure difference between the front and backside of the wafer causes the membrane to bend. A platinum resistor is integrated on top of the membrane and acts both as heater and as temperature sensor. An identical platinum resistor on the substrate is used as a reference sensor. When the membrane is heated by a constant current through the electrical resistor the resulting membrane temperature, with respect to the substrate, is dependent on both the distance from the substrate, i.e. the membrane deflection, and the pressure dependent thermal conductivity of the medium between the membrane and substrate. In principle the thermal readout is suitable for operation at high temperatures, because the temperature difference between the membrane and the substrate is measured, which is in first order approximation independent of the absolute temperature [2]. The deflection of the membrane and the dependency of the thermal conductivity on pressure are depicted in figures 2 and 3.

The thermal resistance between the heated membrane and the substrate can be expressed by:

$$\frac{\Delta T}{Q} = R_{\text{therm}} = \frac{l}{\kappa_f A} \quad (1)$$

with κ_f [$W/(Km)$] the thermal conductivity of the

medium, l [m] the gap distance and A [m²] the area of the membrane. A heating power Q [W] can be applied, which results in a temperature difference ΔT [K] and gives the thermal resistance R_{therm} [K/W].

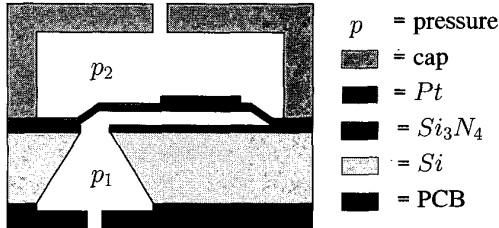


Fig. 1

SCHEMATIC DRAWING OF THE STRUCTURE

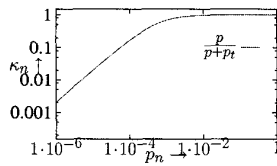


Fig. 2

NORMALIZED THERMAL CONDUCTIVITY VERSUS NORMALIZED PRESSURE

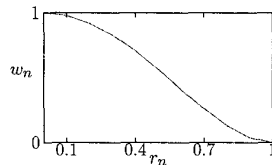


Fig. 3

NORMALIZED DEFLECTION VERSUS NORMALIZED RADIUS

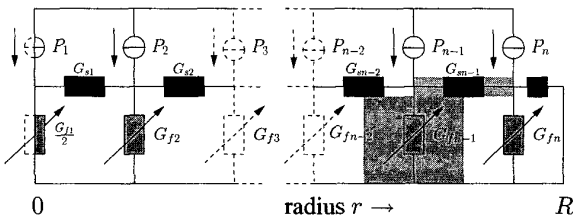


Fig. 4

LUMPED ELEMENT MODEL USED FOR CALCULATING THE TEMPERATURE DISTRIBUTION OF A DEFLECTED MEMBRANE.

The temperature distribution over the membrane is defined by the ratio between the heat transport through the medium and the heat transport through the membrane to the edge of the membrane. The temperature distribution can be obtained by solving the following one dimensional differential equation:

$$-h\kappa_s \left(\frac{d^2T}{dr^2} + \frac{1}{r} \frac{dT}{dr} \right) + \frac{\kappa_f}{l} T = Q'' \quad (2)$$

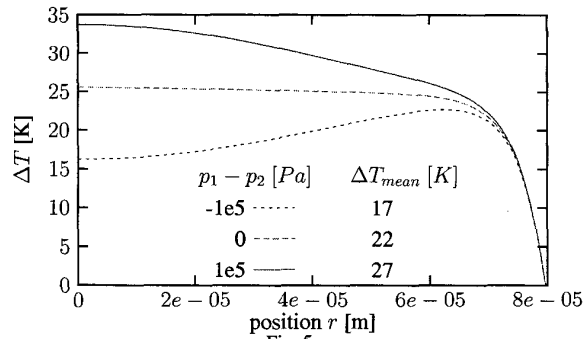


Fig. 5

CALCULATED TEMPERATURE DISTRIBUTION

with κ_s and κ_f the thermal conductivity of the solid membrane and fluid, respectively, and Q'' [W/m²] the applied heating power per unit area.

Using the boundary conditions $T(R) = 0$ and $\frac{T(0)}{dr} = 0$ and taking for the thermal square conductance $G_f'' = \frac{\kappa_f}{l}$ [W/(Km²)] and the thermal square resistance of the membrane $R_s'' = \frac{1}{\kappa_s h}$ [K/W] the solution becomes:

$$T(r) = \frac{Q''}{G_f''} \left(1 - \frac{BesselJ_0 \left(r \sqrt{-G_f'' R_s''} \right)}{BesselJ_0 \left(R \sqrt{-G_f'' R_s''} \right)} \right) \quad (3)$$

with R [m] the radius of the membrane. This solution is plotted in figure 5 as the center curve with $p_1 - p_2 = 0$ [Pa]. When a pressure difference $p_1 - p_2$ [Pa] is applied over the membrane it will bend and the gap distance l changes. For a circular membrane with radius R [m] the deflection w [m] is given by [6]:

$$w(r) = \frac{3}{16} \frac{1 - \nu^2}{E h^3} (R^2 - r^2)^2 \cdot \Delta p \quad (4)$$

with ν the Poisson ratio, E [Pa] the Young's modulus, h [m] the thickness, Δp [Pa] the pressure drop and r [m] the radius from the center of the membrane.

For a deflected membrane the differential equation 2 becomes nonlinear and is difficult to solve. Instead, the lumped element model, indicated in figure 4, was used to calculate the temperature distribution. In this model the heat conductance through the membrane is represented by the conductances G_s [W/(K)]. An expression can be obtained from the heat equation without heat generation using cylindrical coordinates.

$$\frac{1}{r} \frac{d}{dr} \left(\kappa r \frac{dT}{dr} \right) = 0 \quad (5)$$

Combining its solution with Fourier's law results in

$$G_s(i) = \frac{2\pi h\kappa_s}{\ln\left(\frac{r_{i+1}}{r_i}\right)} \quad (6)$$

with n the number of elements

For the thermal conductance of the beam a singularity exists for $r = 0$. Therefore a small value has been taken. The heat conductance through the fluid to the substrate is modeled by the conductances G_f [$W/(K)$], which are dependent on the membrane deflection. The expression is

$$G_f(i) = \kappa_f \frac{\pi R^2}{l} (r_i^2 - r_{i-1}^2) \quad (7)$$

and for the power

$$Q(i) = 2\pi R^2 Q'' (r_i^2 - r_{i-1}^2) \quad (8)$$

Numerical results are shown in figure 5.

Due to the Pirani effect the thermal conductance of the fluid G_f becomes dependent on the pressure, when the distance between the heated membrane and the substrate is smaller than the mean free path of the gas molecules. Around atmospheric pressure this effect becomes noticeable when the distance is in the order of $1 \mu\text{m}$. The Pirani effect can easily be included in the lumped model by making the conductances G_f dependent on both the membrane deflection and the absolute pressure beneath the membrane.

III. FABRICATION PROCESS

In [3] a sacrificial poly-Si layer of about 1 mm long and $1 \mu\text{m}$ high between two silicon nitride layers was etched open by KOH etching from the backside of the wafer. In this way we have realized silicon nitride membranes on the surface of the wafer with the cavity between it connected by a channel to the etch opening at the backside of the wafer. The hole at the backside can easily be closed or connected to a tube. An important advantage compared to other sacrificial layer processes is that it is not necessary to seal etching channels needed to have access to the sacrificial layer.

Membrane diameters from 80 to $240 \mu\text{m}$ were used. The thickness was $1 \mu\text{m}$. The gap between membrane and heat sink was $1 \mu\text{m}$. The metal heater/sensor on top of the membrane consists of a 10 nm Cr adhesion layer and a 200 nm Pt layer, with a width and spacing between the lines of $5 \mu\text{m}$. Note that the same fabrication process can be used to realize a strain gauge or capacitive readout simply by changing the platinum pattern. Different readout principles can even be combined on a single chip.

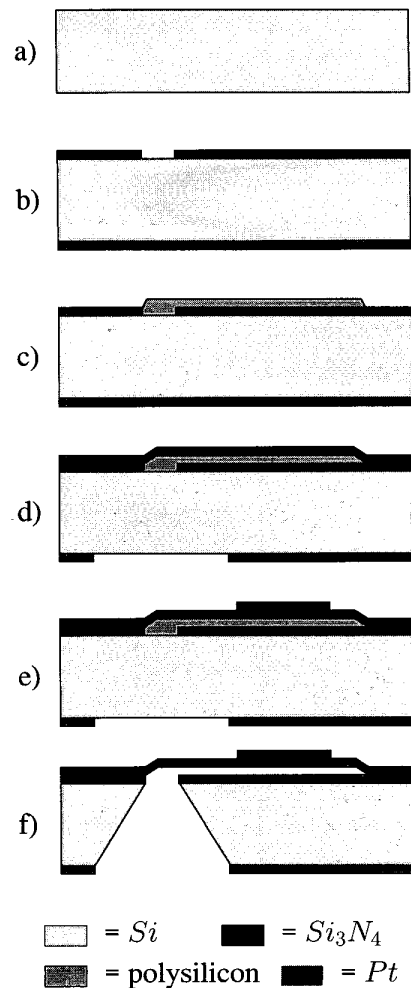


Fig. 6
PROCESS OUTLINE

Figure 6 shows a summary of the fabrication process. On a bare silicon $\langle 100 \rangle$ wafer (a) a $1 \mu\text{m}$ Si_3N_4 layer has been deposited and patterned (b). A sacrificial $1 \mu\text{m}$ polysilicon layer is used for defining the gap (c). Next, a $1 \mu\text{m}$ Si_3N_4 layer is deposited, which forms the membrane. The other side is patterned (d). The 10 nm Cr adhesion layer and the 200 nm Pt are sputtered and patterned by lift-off (e). The last step is the etching in KOH (f).

Figure 7 shows a photograph of the pressure sensor with meandering heater and distributed temperature sensing. Based on the same idea, a Pirani sensor and a flow sensor are presented in [7].

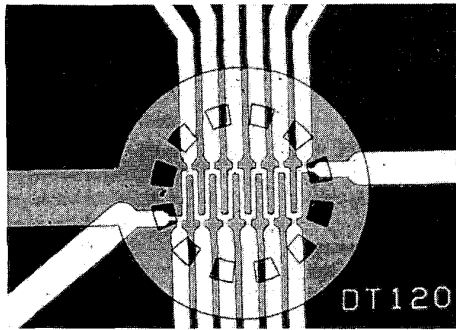


Fig. 7

PHOTOGRAPH OF PRESSURE SENSOR. THE DIAMETER OF THE MEMBRANE IS 120 μm .

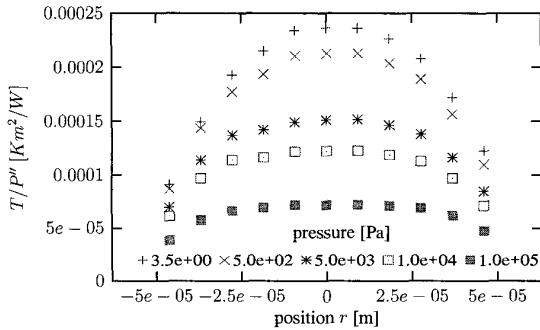


Fig. 8

MEASURED TEMPERATURE DISTRIBUTION VERSUS POSITION FOR SEVERAL UNDERPRESSURES

IV. MEASUREMENTS

The temperature distribution versus the position on the membrane has been measured in a vacuum chamber for pressures ranging from 3.5 Pa up to 1 bar, see figure 8. To keep the temperature rise constant the current has been adapted for each pressure. Therefore the temperature has been divided by the (square) power to be able to compare those.

For the next measurements the membrane was heated with a constant current of 3 mA and the resistance of the heater was approximately 125 Ω . This resulted in a temperature rise of about 8 K. The temperature of the center segment was measured as a function of the pressure difference Δp that was applied above ($p_2 - p_1$), below ($p_1 - p_2$) or at both sides ($p_1 = p_2$) of the membrane, see figure 9. For curve $p_2 - p_1$ we see that the temperature de-

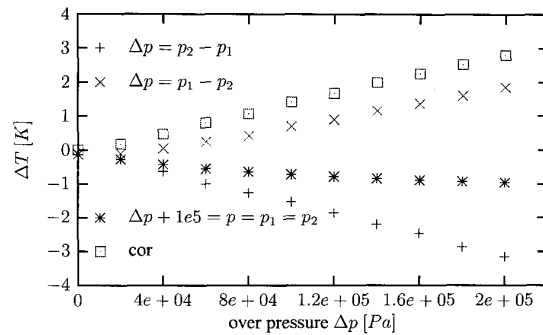


Fig. 9

MEASURED TEMPERATURE CHANGE AS A FUNCTION OF THE PRESSURE DROP APPLIED OVER THE MEMBRANE

creases almost linearly with increasing pressure. In this case the pressure between the membrane and substrate remains constant and the Pirani effect can be neglected. When the same pressure is applied on both sides of the membrane, curve $p_1 = p_2$, the membrane will not deflect. In this case we see that again the temperature decreases with increasing pressure, however the effect is nonlinear because for the gap distance of 1 μm the Pirani effect decreases significantly around atmospheric pressure. A smaller gap distance will result in a much larger and more linear Pirani effect. When the pressure is applied below the membrane, curve $p_1 - p_2$, we have a combination of the Pirani effect, which causes a decrease of the temperature, and an upward deflection of the membrane, which causes an increase of the temperature due to the larger distance from the substrate. Correcting curve $p_1 - p_2$ for the change in thermal conductivity with curve $p_1 = p_2$ gives curve *cor*. The latter is (apart from the sign) almost identical to $p_2 - p_1$ showing that the membrane deflection is symmetrical.

The temperature distribution for several pressures have been measured for a pressure difference that decreases the gap, see figure 10. A dip appears due to the smaller distance to the heat sink at the center. The temperature distribution for an over pressure on both sides is shown in figure 11. Applying the pressure from below results in the temperature distributions of figure 12. Normalizing the temperature distribution of figure 10 to the center segments shows the change of the shape of the curve better, see figure 13. This gives also the possibility to eliminate the temperature coefficient of resistance [7]. Maybe even taking the ratio of two segments, for example one at the center and the other at a quarter of the beam, could be

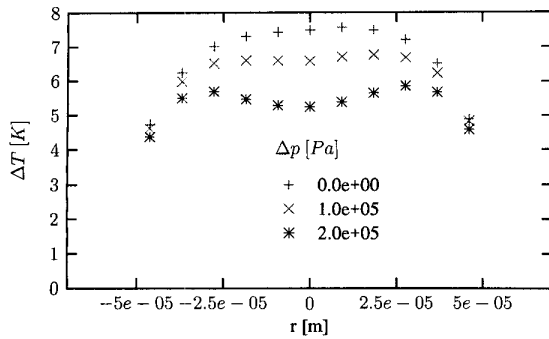


Fig. 10

MEASURED TEMPERATURE DISTRIBUTION VERSUS POSITION FOR SEVERAL OVERPRESSURES

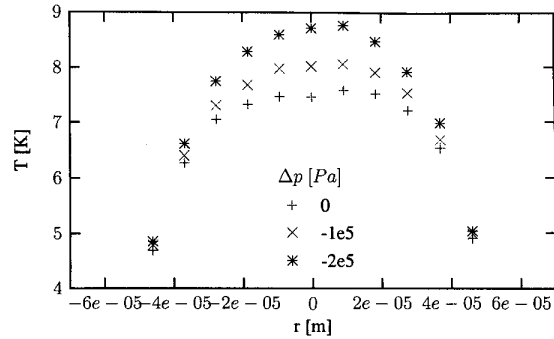


Fig. 12

MEASURED TEMPERATURE CHANGE AS A FUNCTION OF THE PRESSURE DROP APPLIED OVER THE MEMBRANE

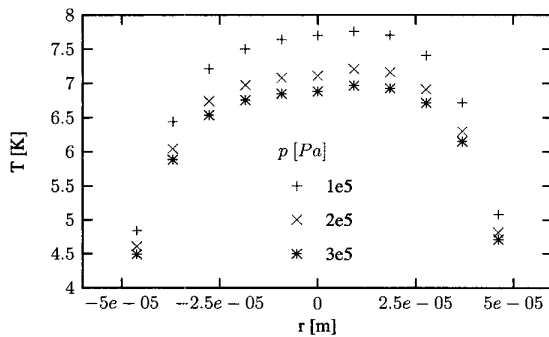


Fig. 11

MEASURED TEMPERATURE DISTRIBUTION VERSUS POSITION FOR SEVERAL ABSOLUTE PRESSURES APPLIED TO BOTH SIDES

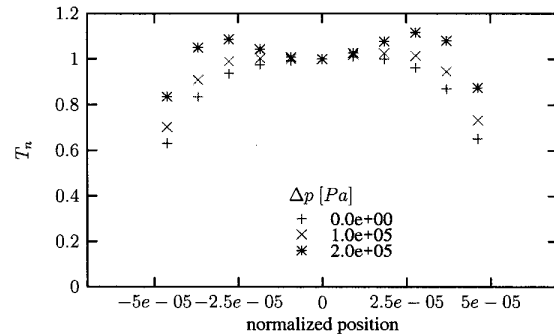


Fig. 13

PLOT OF FIGURE 10 NORMALIZED TO THE TEMPERATURE RISE OF THE CENTER SEGMENT THAT MAKES IT INDEPENDENT OF THE TCR

sufficient.

V. CONCLUSIONS

A combined Pirani/bending membrane pressure sensor with distributed temperature sensing has been realized. First measurement results show that the sensor is sensitive to both a pressure difference (causing a deflection of the membrane) and the absolute pressure between the membrane and the substrate. It was shown that there is a possibility to do the measurements independent of the temperature coefficient of resistance of the sensing elements.

ACKNOWLEDGMENT

This research was funded by the Dutch Technology Foundation (STW).

REFERENCES

- [1] O. Paul. Vacuum gauging with complementary metal-oxide semiconductor microsensors. *J. Vac. Sci. Technol.*, A 13(3):503-508, 1995.
- [2] U.A. Däuerstadt, C.M.A. Ashruf, and P.J. French. A new high temperature pressure sensor based on a thermal read-out principle. *Transducers*, pages 525-530, 1999.
- [3] Xing Yang, Yu-Chong Tai, and Chih-Ming Ho. Micro bellow actuators. *Transducers*, pages 45-48, 1997.
- [4] J.W. Berenschot, N.R. Tas, T.S.J. Lammerink, M. Elwenspoek, and A. van den Berg. Advanced sacrificial poly-si technology for fluidic systems. *Transducers '01 Munich Germany*, 2001.
- [5] J.J. van Baar, R.J. Wiegink, T.S.J. Lammerink, J.W. Berenschot, G.J.M. Krijnen, and M. Elwenspoek. Combined -pirani/bending membrane-pressure sensor. *MEMS Las Vegas*, 2002.
- [6] M. Elwenspoek and R.J. Wiegink. *Mechanical microsensors*. Springer Verlag, 2000.
- [7] J.J. van Baar, R.J. Wiegink, T.S.J. Lammerink, G.J.M. Krijnen, and M. Elwenspoek. Micro-machined structures for thermal measurements of fluid and flow parameters. *J. of MicroMech. and MicroEng.*, volume 11, issue 4 (July):311-318, 2001.